Langmuir

Research Article

Anion Effect on the Nanostructure of a Metal Ion Binding Self-Assembling Peptide

H. Yang, M. Pritzker, S. Y. Fung, Y. Sheng, W. Wang, and P. Chen

Langmuir, **2006**, 22 (20), 8553-8562 • DOI: 10.1021/la061238p

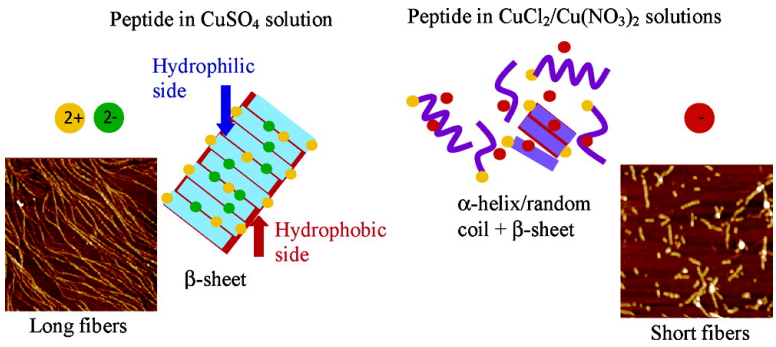

More About This Article

Additional resources and features associated with this article are available within the HTML version:

- Supporting Information
- Links to the 6 articles that cite this article, as of the time of this article download
- Access to high resolution figures
- Links to articles and content related to this article
- Copyright permission to reproduce figures and/or text from this article

View the Full Text HTML

Anion Effect on the Nanostructure of a Metal Ion Binding Self-Assembling Peptide

H. Yang,† M. Pritzker,† S. Y. Fung,† Y. Sheng,‡ W. Wang,‡ and P. Chen*,†

Department of Chemical Engineering, University of Waterloo, 200 University Avenue West, Waterloo, Ontario N2L 3G1, Canada, and National Laboratory of Solid State Microstructure and Department of Physics, Nanjing University, 210093, China

Received May 3, 2006. In Final Form: July 12, 2006

Effects of copper salts containing different anions (SO_4^{2-}, Cl^-, and NO_3^-) on the self-assembly of a designed peptide EAK16(II)GGH with affinity for Cu^{2+} have been investigated. The peptide secondary structure, self-assembled nanostructures, and surface activity were observed to depend strongly on the type of anion. Over a salt concentration range from 0.05 to 10.0 mM, SO_4^{2-} induced long fiber formation, whereas Cl^- and NO_3^- caused short fiber formation. The fiber length increased with copper sulfate concentration, but the concentration of copper chloride and copper nitrate did not affect the peptide nanostructures significantly. Analysis by Fourier transform infrared spectroscopy (FTIR) revealed that the addition of the copper salts tended to cause the peptide conformation to change from α-helix/random coil to β-sheet, the extent to which depended on the anion type. This evidence of the anion effect was also supported by surface tension measurements using the axisymmetric drop shape analysis-profile (ADSA-P) technique. An explanation for the effect of anions on the peptide self-assembly was proposed. The divalent anion SO_4^{2-} might serve as a bridge by electrostatically interacting with two lysine residues from different peptide molecules, promoting β-sheet formation. The extensive β-sheet formation may further promote peptide self-assembly into long fibers. On the other hand, monovalent anions Cl^- and NO_3^- may only electrostatically interact with one charged residue of the peptide; hence, a mixed secondary structure of α-helix/random coil and β-sheet was observed. This observation might explain the predominant formation of short fibers in copper chloride and copper nitrate solutions.

Introduction

Molecular self-assembly is a widely recognized phenomenon in nature. Under certain conditions, amphiphilic molecules can spontaneously assemble into aggregates with a certain size and structure. Self-assembling peptides are a novel class of amphiphilic molecules that are relatively easy to design and synthesize. In recent years, considerable advances have been made in the use of self-assembled nanostructures of these synthetic peptides as building blocks for functional biomaterials.[1,2] These biomaterials have many potential applications such as templates for nanowire fabrication,[3−7] platforms or scaffolds for tissue engineering,[8−10] delivery of proteins and peptide medicines,[11,12] and biological surface engineering.[13]

Among the new class of self-assembling peptides are ionic-complementary peptides, whose sequence motif was serendipitously discovered from a Z-DNA binding protein in yeast.[10] These small peptides contain alternating hydrophobic and hydrophilic residues in sequence and possess a unique property of ionic complementarity. In solution, they can self-assemble into various nanostructures not only through hydrogen bonding but also through electrostatic and hydrophobic interactions. Most of these peptides, such as EAK16-I and EAK16-II, readily self-assemble to form stable nanofibers that have been shown to resist degradation in acidic or alkaline environments.[10,14,15] The size and unusual stability of these nanofibers under extreme solution conditions make these peptides promising materials for applications in nanotechnology. In particular, the possibility of fabricating conductive nanowires using self-assembled peptide nanostructures as templates is of special interest to the electronics industry. The "bottom-up" nanofabrication technique based on molecular self-assembly to construct supermolecules from single molecules can overcome the various limitations of traditional "top down" (an approach starting from large-scale operation) approaches, such as optical lithography.[1] These top-down methods have approached their physical limits of resolution due to constraints mainly arising from the wavelength of the optical sources and quantum mechanical effects.[16] In addition, increasing costs also impede the further scaling down of conventional silicon technology.[17] The search for alternative technologies for metallic nanowire and electronic device fabrication has stimulated a considerable amount of research interest.[6,7,18−23]

† University of Waterloo.
‡ Nanjing University.
* Corresponding author. E-mail: p4chen@cape.uwaterloo.ca.

(1) Zhang, S.; Marini, D. M.; Hwang, W.; Santoso, S. *Curr. Opin. Chem. Biol.* **2002**, *6*, 865−871.
(2) Zhang, S. *Nat. Biotechnol.* **2003**, *21*, 1171−1178.
(3) Yu, L.; Banerjee, I. A.; Shima, M.; Rajan, K.; Matsui, H. *Adv. Mater.* **2004**, *16*, 709−712.
(4) Banerjee, I. A.; Yu, L.; Matsui, H. *Proc. Natl. Acad. Sci. U.S.A.* **2003**, *100*, 14678−14682.
(5) Yu, L.; Banerjee, I. A.; Matsui, H. *J. Mater. Chem.* **2004**, *14*, 739−743.
(6) Reches, M.; Gazit, E. *Science* **2003**, *300*, 625−627.
(7) Scheibel, T.; Parthasaarathy, R.; Sawicki, G.; Lin, X.-M.; Jaeger, H.; Lindquist, S. L. *Proc. Natl. Acad. Sci. U.S.A.* **2003**, *100*, 4527−4532.
(8) Holmes, T. C.; de Lacalle, S.; Su, X.; Liu, G.; Rich, A.; Zhang, S. *Proc. Natl. Acad. Sci. U.S.A.* **2000**, *97*, 6728−6733.
(9) Zhang, S.; Holmes, T.; Lockshin, C.; Rich, A. *Proc. Natl. Acad. Sci. U.S.A.* **1993**, *90*, 3334−3338.
(10) Zhang, S.; Holmes, T.; DiPersio, C. M.; Hynes, R. O.; Su, X.; Rich, A. *Biomaterials* **1995**, *16*, 1385−1393.
(11) Aggeli, A.; Boden, N.; Zhang, S. *Mol. Med. Today* **1999**, *5*, 512−513.
(12) Zhang, S.; Altman, M. *React. Funct. Polym.* **1999**, *41*, 91−102.
(13) Zhang, S.; Yan, L.; Altman, M.; Lassle, M.; Nugent, H.; Frankel, F.; Lauffenburger, D. A.; Whitesides, G. M.; Rich, A. *Biomaterials* **1999**, *20*, 1213−1220.
(14) Fung, S. Y.; Keyes, C.; Duhamel, J.; Chen, P. *Biophys. J.* **2003**, *85*, 537−548.
(15) Hong, Y.; Legge, R. L.; Zhang, S.; Chen, P. *Biomacromolecules* **2003**, *4*, 1433−1442.
(16) Stoltenberg, R. M.; Woolley, A. T. *Biomed. Microdevices* **2004**, *6*, 105−111.
(17) He, H.; Tao, N. J. in *Encyclopedia of Nanoscience and Nanotechnology*; Nalwa, H. S., Ed.; American Scientific Publishers: Stevenson Ranch, CA, 2004; Vol. 2, p 755.

10.1021/la061238p CCC: $33.50
Published on Web 09/02/2006

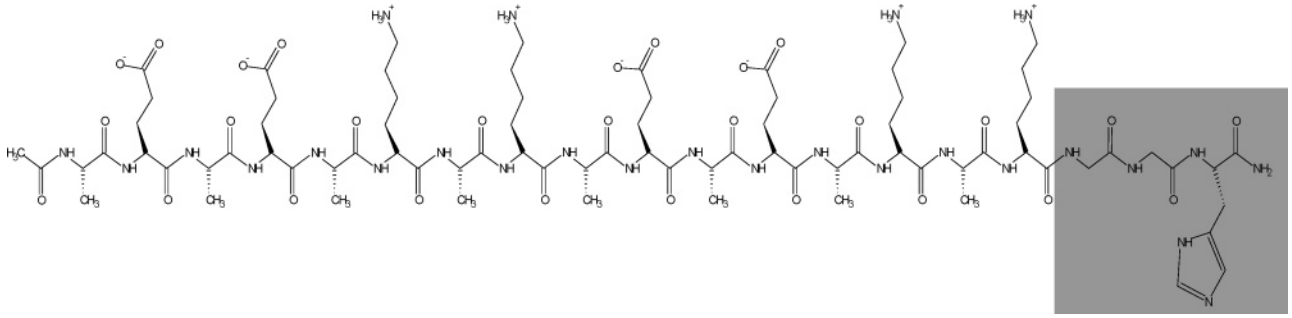

Figure 1. Schematic diagram of EAK16(II)GGH structure. The gray portion shows the functional GGH group.

One important application of peptide self-assembled nanofibers is to act as templates for metallic nanowire fabrication.[6,7,24] Our current effort in this direction focuses on the production of nanowires from copper due to its widespread use in the electronics industry. Our strategy is to incorporate copper into the nanofibers via a metal binding site in a self-assembling peptide. EAK16-II, an ionic-complementary peptide well-known for its ability to self-assemble into nanofibers, has been chosen to serve as the model peptide. It is modified by adding a functional Cu^{2+} binding group GGH[25] (G, glycine; H, histidine) to the C-terminus of EAK16-II. The molecular structure of this newly designed peptide, called EAK16(II)GGH, is shown in Figure 1. GGH has been chosen as the metal binding group and located at the C-terminus for the following reasons: (1) it can provide nitrogen donors to coordinate with Cu^{2+} in a tetragonal geometry[26,27] and is not expected to significantly affect the self-assembly of EAK16-II into nanofibers due to its small size, and (2) GGH has been shown from quantum mechanical calculations to have a higher binding constant for Cu^{2+} than other tripeptides.[26] Thus, the designed peptide may bind with copper strongly and the metal−peptide complex may have high stability, an important factor for the later metallization of the peptide nanofiber.

During preliminary experiments, it became apparent that the type of Cu^{2+} salt present has a strong impact on the geometry of the peptide self-assembled nanostructures. This paper describes the results of a detailed experimental study on the influence of SO_4^{2-}, Cl^-, and NO_3^- anions on the molecular structure, self-assembled nanostructure, and thermodynamic behavior of the newly designed peptide EAK16(II)GGH. The binding of EAK16-(II)GGH to Cu^{2+} was characterized by nuclear magnetic resonance (NMR) and UV−vis absorption spectroscopy. The peptide secondary structure was characterized by Fourier transform infrared spectroscopy (FTIR). The nanostructures of the peptide assemblies were observed using atomic force microscopy (AFM). Since EAK16(II)GGH has an amphiphilic structure and surfactant-like properties similar to EAK16s,[14,15,28] with hydrophilic residues on one side and hydrophobic residues on the other side, the self-assembled nanostructure may also exhibit such amphiphilicity. Thus, the surface tensions of solutions containing EAK16(II)GGH and the copper salts were measured using the axisymmetric drop shape analysis-profile (ADSA-P) technique. Surface tension can be used to assess the surface activity of peptide assemblies and kinetics of peptide adsorption at surfaces.

Experimental Section

Materials. The self-assembling peptide EAK16(II)GGH ($C_{80}H_{134}N_{26}O_{28}$, molecular weight 1908 g mol^{-1}) has a sequence of AEAEAKAKAEAEAKAKGGH (see Figure 1) where A corresponds to alanine, E to glutamic acid, K to lysine, G to glycine, and H to histidine. At neutral pH, A and G are neutral hydrophobic residues, whereas E is a negatively charged hydrophilic residue, K is positively charged, and H may be partially charged since its normal pK_a is about 6.0. The real pK_a value of histidine in a specific peptide or protein can be changed by the formation of a peptide bond,[29] terminal modification,[30] the location,[31,32] and the interaction with other amino acids.[31] The proportion of charged histidine groups can be expressed as $10^{(pK_a-pH)}/[1 + 10^{(pK_a-pH)}]$. This peptide was purchased from Invitrogen (Burlington, Canada) with a purity of >95% (purified by reverse-phase high-performance liquid chromatography). The N-terminus and C-terminus of the peptide were protected by acetyl and amino groups, respectively, to minimize end-to-end electrostatic attraction between peptides.[28]

Peptide solutions were freshly prepared in pure water (18.2 MΩ; Millipore Milli-Q system) and copper salt stock solutions (from 0.05 mM to 10.0 mM) at concentrations of 0.025 and 0.05 mg mL^{-1} (12.4 and 24.8 μM EAK16(II)GGH). To avoid interference from other anions, a buffer solution was not used to control pH. However, in the copper binding experiments, a minute amount of NaOH was used to adjust the solution pH to 6.0 to enable the binding of copper to peptide molecules and to stabilize the chemical shift of protons (see below). At a peptide concentration of 0.05 mg mL^{-1}, the pH measured in the presence of 1.0 mM copper salts without the addition of NaOH was about 5.9 regardless of the anion present, whereas the pH was 6.2 in the absence of the salt. The ionic strength of the solutions was not further adjusted by the addition of any other electrolyte to avoid interference from other ions. All peptide solutions were stored at 4 °C before use. Copper sulfate, copper chloride, copper nitrate, sodium sulfate, and sodium chloride (Sigma-Aldrich, Oakville, Canada) with purity of 99.9+ % were used in the experiments.

Nuclear Magnetic Resonance (NMR). The ^{1}H NMR spectra were acquired at 25 °C on a Bruker Avance DMX 600 MHz spectrometer equipped with a triple resonance *xyz*-gradient probe

(18) Djalali, R.; Chen, Y.; Matsui, H. *J. Am. Chem. Soc.* **2002**, *124*, 13660−13661.
(19) Knez, M.; Bittner, A. M.; Boes, F.; Wege, C.; Jeske, H.; Mai, E.; Kern, K. *Nano Lett.* **2003**, *3*, 1079−1082.
(20) Valizadeh, S.; George, J. M.; Leisner, P.; Hultman, L. *Electrochim. Acta* **2001**, *47*, 865−874.
(21) Lee, S.-W.; Mao, C.; Flynn, C. E.; Belcher, A. M. *Science* **2002**, *296*, 892−895.
(22) Cheng, C.; Gonela, R. K.; Gu, Q.; Haynie, D. T. *Nano Lett.* **2005**, *5*, 175−178.
(23) Braun, E.; Eichen, Y.; Sivan, U.; Ben-Yoseph, G. *Nature* **1998**, *391*, 775−778.
(24) Djalali, R.; Chen, Y.; Matsui, H. *Polym. Mater.: Sci., Eng.* **2003**, *88*, 29−30.
(25) Yang, W.; Jaramillo, D.; Gooding, J. J.; Hibbert, D. B.; Zhang, R.; Willett, G. D.; Fisher, K. *Chem. Commun.* **2001**, 1982−1983.
(26) Yang, W.; Chow, E.; Willett, G. D.; Hibbert, D. B.; Gooding, J. J. *Analyst* **2003**, *128*, 712−718.
(27) Sanna, D.; Ágoston, C. G.; Sóvágó, I.; Micera, G. *Polyhedron* **2001**, *20*, 937−947.
(28) Jun, S.; Hong, Y.; Immamura, H.; Ha, B.-Y.; Bechhoefer, J.; Chen, P. *Biophys. J.* **2004**, *87*, 1249−1259.
(29) Nozaki, Y.; Tanford, C. *Methods Enzymol.* **1967**, *11*, 715−734.
(30) Tanokura, M. *Biochim. Biophys. Acta* **1983**, *742*, 576−585.
(31) Singer, A. U.; Forman-Kay, J. D. *Protein Sci.* **1997**, *6*, 1910−1919.
(32) Lee, K. K.; Fitch, C. A.; Lecomte, J. T. J.; Garcia-Moreno, B. *Biochemistry* **2002**, *41*, 5656−5667.

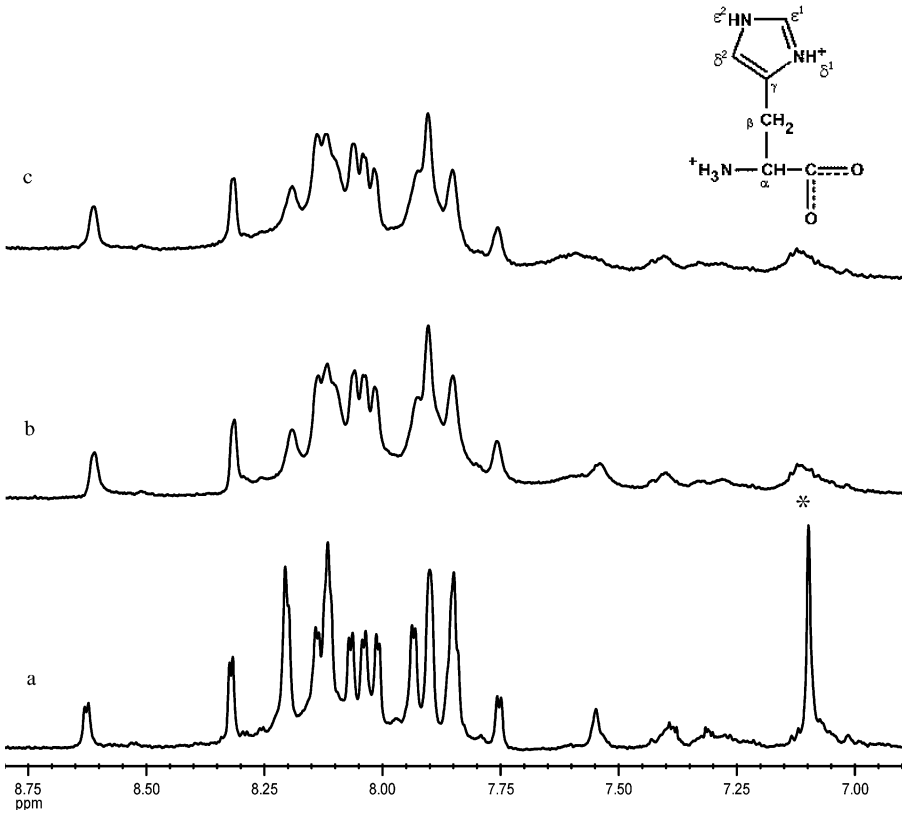

Figure 2. ^{1}H NMR spectra of 1.0 mM EAK16(II)GGH at pH 6.0. The lower spectrum (a) corresponds to EAK16(II)GGH, whereas the upper spectrum (b) corresponds to EAK16(II)GGH with 0.25 mM of $CuCl_2$ titrated in and (c) corresponds to EAK16(II)GGH with 0.25 mM of $CuSO_4$ titrated in. * denotes the signal for the H-δ^2 proton of histidine imidazole side chain. The inset is the structure of histidine.

and processed using Felix 97.0 software (MSI, Inc.). The spectra were recorded using 90% H_2O/10% D_2O solutions, typically at a peptide concentration of 1.0 mM. The pH of the peptide solution was adjusted to 6.0 using small aliquots of 0.1 M NaOH prepared in 90% H_2O/10% D_2O solution. This pH was chosen to prevent the precipitation of $Cu(OH)_2$ (K_{sp} of $Cu(OH)_2 = 1.6 \times 10^{-19}$) and ensure copper binding to histidine. The measured pH values were uncorrected for the isotope effect. In the metal ion binding study, small aliquots (0.25 mM) of $CuCl_2$ and $CuSO_4$ solution were added to the peptide solution, respectively. Correction for the volume change during copper titration was made during the analysis.

UV−Vis Absorption Spectroscopy. The absorption spectra were obtained on a UV−vis spectrophotometer (Biochrom Ultraspec 4300 Pro, Cambridge, England) using a 1 cm path-length quartz cuvette. The copper ion titration was performed by adding small aliquots of $CuCl_2$ or $CuSO_4$ stock solution (70 mM) to 0.6 mg mL^{-1} (0.3 mM) EAK16(II)GGH solution. The final contents of copper ions for each titration ranged from 0.19 to 1.82 mM. The solution pH was adjusted to 6.0 by adding small amounts of 0.1 M NaOH, HCl (for experiments involving $CuCl_2$), or H_2SO_4 (for experiments involving $CuSO_4$). The spectra were smoothed and deconvoluted after background correction using the PeakFit 4.12 software (Hearne Scientific Software LLC, Chicago, IL) to obtain the absorbance of bound copper ions at ∼611 nm.

Fourier Transform Infrared Spectroscopy (FTIR). FTIR spectra over the range from 1600 to 1700 cm^{-1} where the characteristic amide I band appears were obtained to determine the secondary structure of peptide in different copper salt solutions. Examination of this band enables distinction to be made between β-sheets and α-helices/random coils. The peptide (1.0 mM) or peptide/copper salt (1.0 mM) solutions (∼100 μL, incubated for one week to allow secondary structures to form) were placed on a crystal slide of calcium fluoride (CaF_2) and dried at room temperature. The FTIR spectra of the thin films were obtained at a wavenumber resolution of 4 cm^{-1} with a Bio-Rad spectrometer (FTS3000MX, EXCALIBUR series, Hercules, CA). The baseline was subtracted from the observed absorption intensity and the resulting spectrum was normalized with respect to the maximum intensity.

Atomic Force Microscopy (AFM). The nanostructures formed by self-assembly of the peptide in pure water and the copper salt solutions were characterized by AFM. Approximately 10 μL of sample solution was placed on the surface of a freshly cleaved mica sheet fixed to a steel AFM sample plate. The sample was then covered by a Petri-dish to avoid dust and allowed to settle for 10 min to allow the peptide to adhere onto the mica surface. It was then rinsed twice with ∼50 μL of pure water to remove any unattached peptides and salt components before being air-dried for 3 h. Imaging was performed at room temperature on a PicoScan AFM (Molecular Imaging, Phoenix, AZ) using the tapping mode. This mode was used in order to reduce sample surface distortion due to tip and sample interactions. All images were acquired using a 225 μm silicon single-crystal cantilever (NCL type, Molecular Imaging, Phoenix, AZ) with a typical tip radius of 10 nm and resonance frequency of ∼170 kHz. A scanner with the maximum scan size of $6 \times 6\ \mu m^2$ was used. All AFM images were obtained at a resolution of 512 × 512 pixels on a scale of $2\ \mu m \times 2\ \mu m$. All the peptide fiber widths reported herein were corrected using the deconvolution method reported by Fung et al.[14] The actual fiber width W^* can be calculated from the equation $W^* = W - 2[H(2R_c - H)]^{1/2}$, where W is the apparent fiber width from the AFM image, H is the height of the fiber, and R_c (10 nm) is the AFM tip radius. The dimensions of at least 50 fibers were measured at each concentration of peptide and copper salts to obtain the average fiber widths and heights. Fiber lengths were determined using the point-and-click measurement tool available with the PicoScan software. When a fiber was curved, a series of lines was used to trace the fiber axis and then all of the individual line segments were added to yield the fiber length. At least 100 fibers were measured for each solution condition (concentration of peptide and copper salts) to obtain the distribution of the fiber lengths. The frequencies of the fiber length at the following size ranges were determined to generate the distribution histogram: very short fibers (<300 nm),

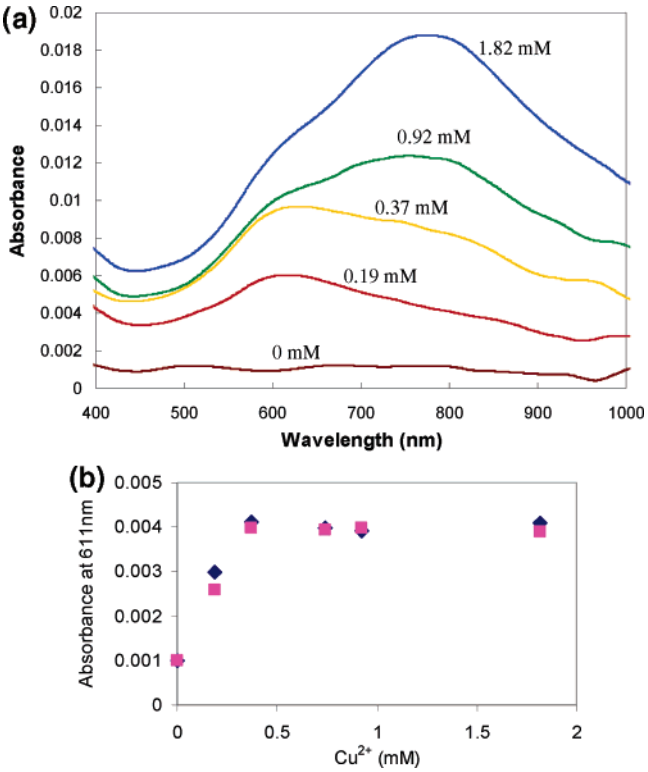

Figure 3. UV−vis spectra resulting from Cu^{2+} titration of 0.6 mg mL^{-1} EAK16(II)GGH (0.3 mM) at pH 6.0. Absorbance spectra of EAK16(II)GGH titrated with increasing concentrations of $CuCl_2$ are shown in panel a. A plot of the deconvoluted absorbance at 611 nm versus increasing concentrations of $CuCl_2$ (solid diamond) and $CuSO_4$ (solid square) are shown in panel b.

short fibers (300−500 nm), intermediate fibers (500−1000 nm), and long fibers (>1000 nm).

Surface Tension Measurement. The experimental setup of the ADSA-P technique to study the dynamic surface tension of EAK16-(II)GGH in pure water and copper salt solutions was described in more detail in an earlier publication.[33] A pendant drop of the peptide solution was formed at the tip of a vertical Teflon needle (0.92 mm inner diameter) connected to a motor-driven microsyringe (1 mL, release speed of 0.04 mL s^{-1}). The sample was placed in a temperature-controlled environmental chamber, saturated with water vapor to maintain consistent humidity. The entire system was placed on a vibration-free table. The images of the pendant drop were magnified by an optical microscope and then captured by a CCD camera before being transferred to a computer. The surface tensions of solutions containing pure copper salts and peptides were measured over the period of 2 and 3 h, respectively. During each run, images were acquired at 0.5 s intervals for the first 70 s and then at 20 s intervals for the remaining time. Software was used to digitize the images and generate a profile of the pendant drop. A theoretical curve governed by the Laplace equation of capillarity was then fitted to the profile, generating the surface tension value as a fitting parameter.[34] The standard deviation of the surface tension values obtained was less than 0.2 mJ m^{-2}.

Results

Copper Binding Study. The effect of Cu^{2+} on the ^1H NMR spectrum of EAK16(II)GGH was studied to obtain evidence for its binding to the peptide. In the absence of Cu^{2+}, one of the aromatic protons of histidine appears at 7.10 ppm, as shown in Figure 2a. This chemical shift has been previously assigned to the H-δ^2 proton of histidine at pH ∼ 6.0.[35] The other aromatic protons are difficult to identify as a result of their overlapping with the amide protons of the peptide. The addition of the paramagnetic ion Cu^{2+} ($CuCl_2$ or $CuSO_4$) to EAK16(II)GGH causes line broadening of the proton resonance in the amide regions. These regions are associated with NH groups from the peptide backbone, histidine, and lysine residues, and the NH_2 group of the C-terminus. The most affected signal belongs to the H-δ^2 proton of histidine (7.10 ppm). The addition of Cu^{2+} to the solution causes this resonance to broaden significantly (Figure 2, panels b and c) and almost disappear. This line broadening is associated with protons close to the paramagnetic ion.[36,37] With such a low level of Cu^{2+} present (0.25 mM), the observation of significant broadening of the resonance of the δ proton of histidine provides evidence for the binding of Cu^{2+} to the histidine residue. In the meanwhile, the selective line broadening of the proton resonance in the amide regions may indicate that some amides in addition to histidine are also involved in the copper binding. The NMR spectra (Figure 2) do not vary depending on whether the anion Cl^- or SO_4^{2-} is present.

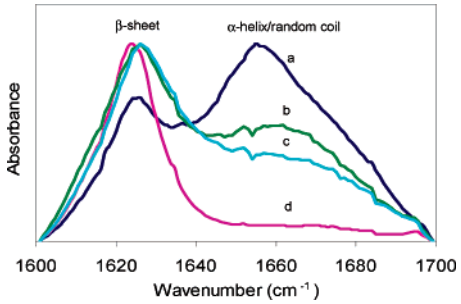

Figure 4. FTIR spectra of EAK16(II)GGH film formed with (a) no salt and in the presence of (b) $CuCl_2$, (c) $Cu(NO_3)_2$, and (d) $CuSO_4$.

The effect of anions on the amount of copper binding to EAK16(II)GGH was studied via UV−vis absorption spectroscopy. As shown in Figure 3a, the addition of Cu^{2+} led to an increase in absorbance in the spectra between 500 and 1000 nm. In this region, the presence of copper led to an absorption band centered at 611 nm for the first 0.19 mM Cu^{2+} and a second feature centered near 800 nm with further increasing Cu^{2+} concentration. The latter band is similar to that observed in pure copper chloride solutions, indicating that it is associated with the free (unbound) copper in solution. Thus, the absorption band at ∼611 nm is associated with the copper−peptide complex. This observation shows evidence of the binding of Cu^{2+} with the peptide EAK16(II)GGH. The plot of the deconvoluted absorption at 611 nm with increasing concentration of $CuCl_2$ and $CuSO_4$ (Figure 3b) shows a linear increase of the absorbance up to 0.37 mM Cu^{2+} before reaching a plateau for both copper salts. The addition of excess Cu^{2+} does not result in a further increase in the absorbance. The presence of different anions (Cl^- and SO_4^{2-}) did not show a significant change in the absorbance of the peptide−copper complexes. This indicates the amount of copper bound to the peptide EAK16(II)GGH was not affected by the presence of different anions, at least to the resolution of the measurement.

Secondary Structure of EAK16(II)GGH. To study the effect of the different copper salts on the peptide conformation, FTIR

(33) Chen, P.; Lahooti, S.; Policova, Z.; Cabrerizo-Vilchez, M. A.; Neumann, A. W. *Colloids Surf. B: Biointerfaces* **1996**, *6*, 279−289.
(34) Rotenberg, Y.; Boruvka, L.; Neumann, A. W. *J. Colloid Interface Sci.* **1983**, *93*, 169−183.
(35) Gaggelli, E.; Bernardi, F.; Molteni, E.; Pogni, R.; Valensin, D.; Valensin, G.; Remelli, M.; Luczkowski, M.; Kozlowski, H. *J. Am. Chem. Soc.* **2005**, *127*, 996−1006.
(36) Tanaka, T.; Mizuno, T.; Fukui, S.; Hiroaki, H.; Oku, J.; Kanaori, K.; Tajima, K.; Shirakawa, M. *J. Am. Chem. Soc.* **2004**, *126*, 14023−14028.
(37) Jones, C. E.; Abdelraheim, S. R.; Brown, D. R.; Viles, J. H. *J. Biol. Chem.* **2004**, *279*, 32018−32027.

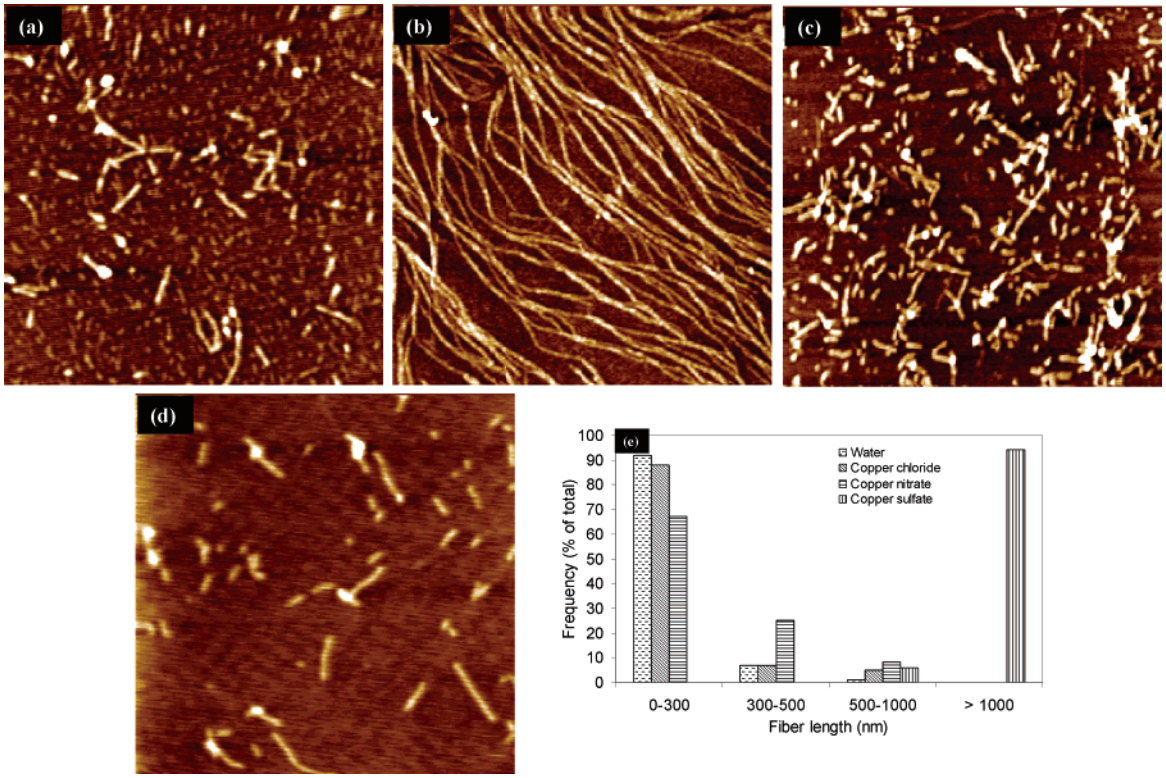

Figure 5. AFM images of nanostructures formed in 0.025 mg mL^{-1} EAK16(II)GGH solutions containing 1.0 mM salts after 4 h incubation time: (a) no salt, (b) $CuSO_4$, (c) $CuCl_2$, (d) $Cu(NO_3)_2$, and (e) histogram of fiber length analysis. The scan area for each image is 2000 nm × 2000 nm.

spectroscopy was used since it can distinguish between β-sheets and α-helices/random coils within the amide I band (1600−1700 cm^{-1}) caused by C═O stretching. Figure 4 shows the FTIR spectra of the amide I band for EAK16(II)GGH samples obtained in the absence and presence of the copper salts. Two characteristic bands appear in these spectra. The peak at about 1626 cm^{-1} can be attributed to the formation of a β-sheet structure.[28,38] The assignment of the band at about 1655 cm^{-1} is complicated since absorbance in this region can arise from α-helix and random coil structures.[39] In the absence of copper salts, a prominent peak appears at 1655 cm^{-1}, revealing that α-helix/random coils form a major portion of the secondary structure. However, a distinct peak also occurs at 1626 cm^{-1} and indicates that β-sheets form as well. The addition of the copper salts causes significant changes to the spectra. In the presence of $CuCl_2$ and $Cu(NO_3)_2$, the absorbance at 1655 cm^{-1} diminishes whereas the 1626 cm^{-1} peak increases relative to that obtained in the salt-free solution. This clearly shows that the salts promote the formation of β-sheets over the other structures. The absorbance at 1655 cm^{-1} is slightly higher when $CuCl_2$ is present than when $Cu(NO_3)_2$ is added. The behavior observed in the presence of $CuSO_4$ differs considerably from that of the other two salts. The absorbance signal for the α-helix/random coil structure disappears entirely and the peak characteristic of a β-sheet structure becomes sharper and shifts slightly toward lower wavenumbers. A shift of approximately 2 cm^{-1} of the β-sheet peak toward lower frequency relative to that observed in the other spectra may reflect an increase in the number of hydrogen bonds.[40] Based on the ratio of the 1626 and 1655 cm^{-1} peak heights, the relative content of β-sheet to α-helix/random coil structures formed in the presence of the different anions can be estimated and follows the order SO_4^{2-} > NO_3^- > Cl^-. $CuSO_4$ is apparently more effective than the other two

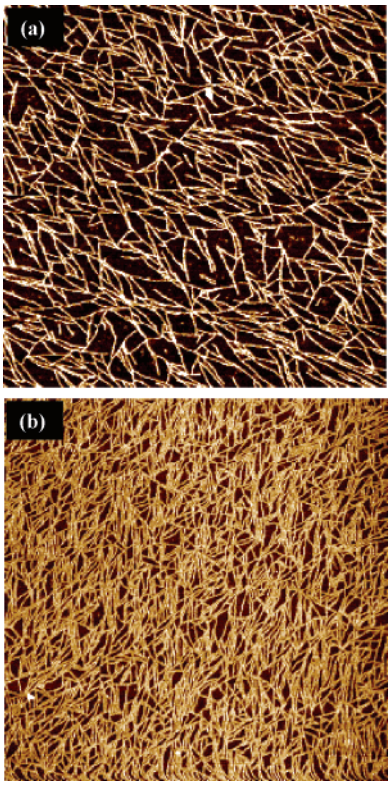

Figure 6. AFM images of nanostructures formed in 0.025 mg mL^{-1} EAK16(II)GGH with solutions containing 1.0 mM (a) Na_2SO_4 and (b) NaCl after 4 h incubation time. The scan area for each image is 2000 nm × 2000 nm.

(38) Casal, H. L.; Köhler, U.; Mantsch, H. H. *Biochim. Biophys. Acta* **1988**, *957*, 11−20.
(39) Lin, S.-Y.; Chu, H.-L. *Int. J. Biol. Macromol.* **2003**, *32*, 173−177.
(40) Gustiananda, M.; Haris, P. I.; Milburn, P. J.; Gready, J. E. *FEBS Lett.* **2002**, *512*, 38−42.

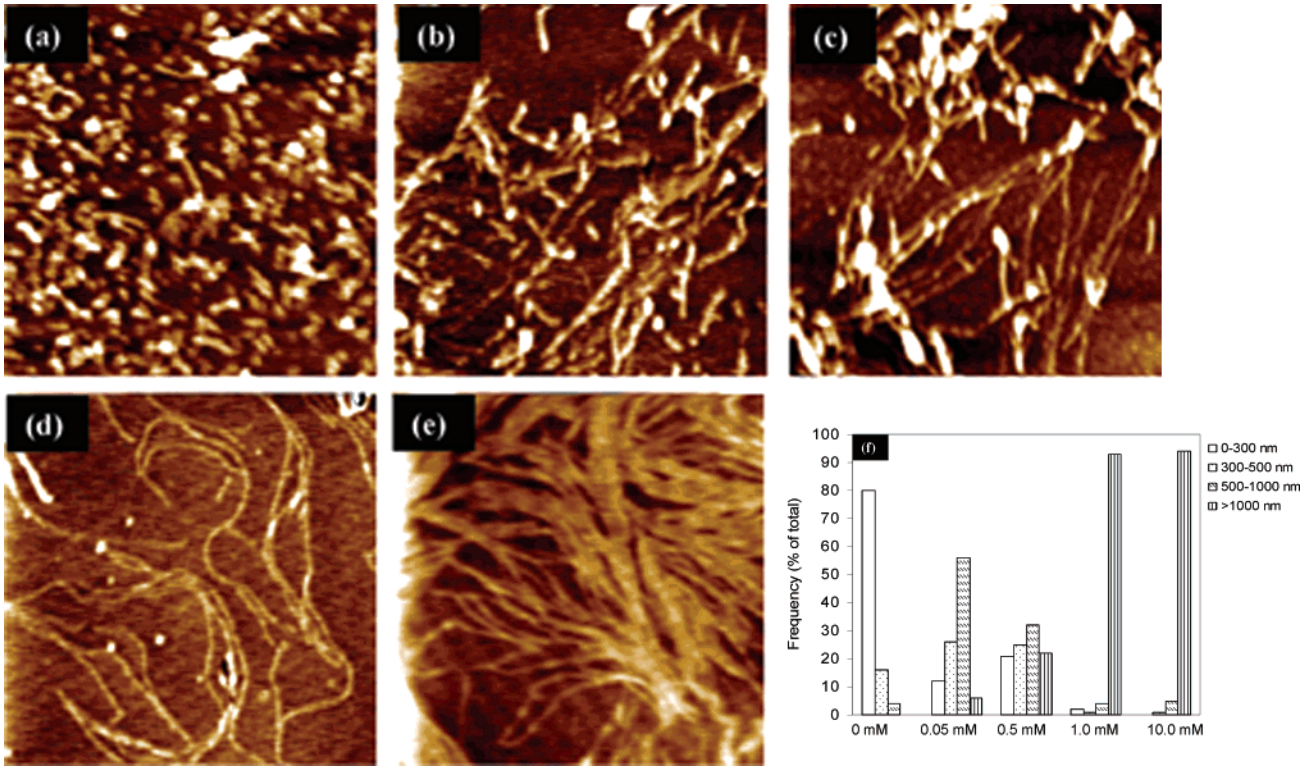

Figure 7. AFM images of nanostructures formed in 0.05 mg mL^{-1} EAK16(II)GGH containing different $CuSO_4$ concentrations after 4 h incubation time: (a) 0, (b) 0.05 mM, (c) 0.5 mM, (d) 1.0 mM, (e) 10.0 mM, and (f) histogram of fiber length analysis. The scan area for each image is 2000 nm × 2000 nm.

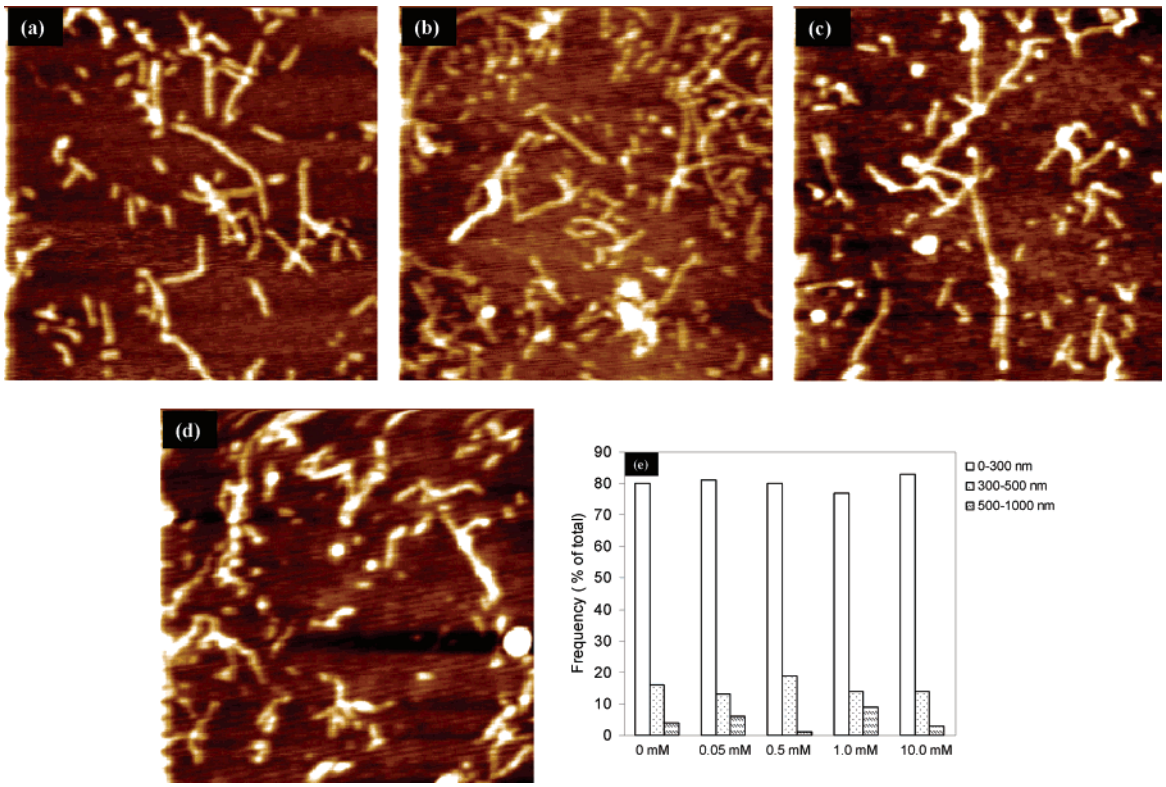

Figure 8. AFM images of nanostructures formed in 0.05 mg mL^{-1} EAK16(II)GGH containing different $CuCl_2$ concentrations after 4 h incubation time: (a) 0.05 mM, (b) 0.5 mM, (c) 1.0 mM, (d) 10.0 mM, and (e) histogram of fiber length analysis. The scan area for each image is 2000 nm × 2000 nm.

salts at promoting the formation of β-sheets to the exclusion of the other secondary structures.

Effect of Anion on Nanostructures. Figure 5 (panels a−d) shows the AFM images of self-assembled nanostructures in solutions containing 0.025 mg mL^{-1} EAK16(II)GGH in the presence and absence of 1.0 mM copper salts. A significant difference in the morphology of the peptide nanostructures is observed depending on the solution composition. In pure water

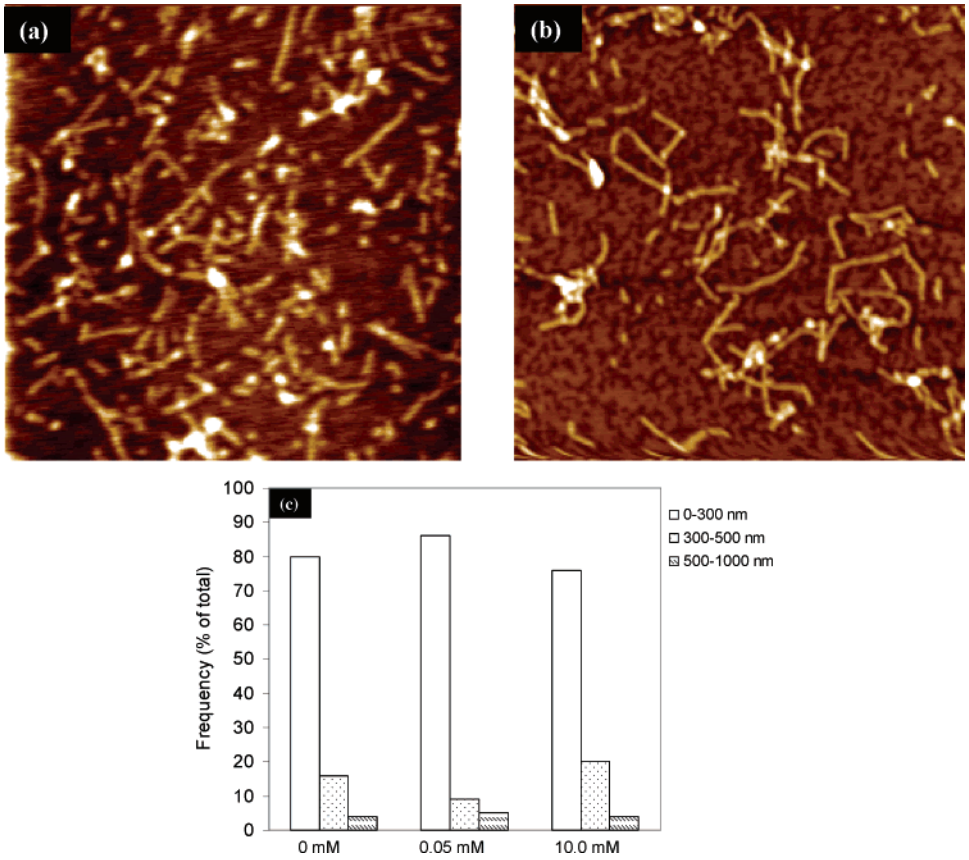

Figure 9. AFM images of nanostructures formed in 0.05 mg mL^{-1} EAK16(II)GGH containing different $Cu(NO_3)_2$ concentrations after 4 h incubation time: (a) 0.05 mM, (b) 10.0 mM, and (c) histogram of fiber length analysis. The scan area for each image is 2000 nm × 2000 nm.

Table 1. Width (W) and Height (H) of EAK16(II)GGH Self-Assembled Nanofibers at Various Conditions

	water		1.0 mM $CuSO_4$		1.0 mM $CuCl_2$		1.0 mM $Cu(NO_3)_2$	
peptide (mg mL^{-1})	W (nm)	H (nm)	W (nm)	H (nm)	W (nm)	H (nm)	W (nm)	H (nm)
0.025	41.5 ± 8.5	1.0 ± 0.20	36.4 ± 5.8	0.5 ± 0.1	38.8 ± 7.0	0.9 ± 0.2	50.0 ± 6.4	0.6 ± 0.1
0.05	56.3 ± 8.3	0.6 ± 0.1						

		$CuSO_4$		$CuCl_2$		$Cu(NO_3)_2$	
peptide (mg mL^{-1})	salt (mM)	W (nm)	H (nm)	W (nm)	H (nm)	W (nm)	H (nm)
0.05	0.05	63.8 ± 14.3	0.6 ± 0.2	59.8 ± 9.3	0.6 ± 0.1	51.5 ± 11.4	0.6 ± 0.1
	0.5	58.2 ± 8.3	0.8 ± 0.3	60.9 ± 9.9	0.4 ± 0.1		
	1.0	51.7 ± 9.4	0.5 ± 0.2	68.1 ± 12.2	0.5 ± 0.1		
	10.0	58.7 ± 7.8	0.4 ± 0.1	63.7 ± 11.2	0.6 ± 0.2	49.7 ± 8.8	0.8 ± 0.2

(Figure 5a), copper chloride (Figure 5c), and copper nitrate (Figure 5d) solutions, the peptide tends to form randomly dispersed short fibers and a few small aggregates, whereas elongated fibers are formed in copper sulfate solution (Figure 5b). This phenomenon is also observed at a higher peptide concentration of 0.05 mg mL^{-1} and over salt concentrations ranging from 0.05 to 10.0 mM (Figures 7−9). The dimensions of the EAK16(II)GGH nanofibers shown in the AFM images (Figure 5a−d) are summarized in Table 1. The peptide forms ribbonlike structures in pure water and copper salt solutions, as reflected in the fiber dimensions (the fiber width is much larger than the fiber height). No significant changes in the fiber width and height are found in the different solutions. The average fiber widths and heights vary from 40 to 50 nm and 0.5 to 1.0 nm, respectively (Table 1). Statistical analysis in Figure 5e shows that the percentage of fibers that lie in the very short range (<300 nm) are 92%, 88%, and 67% in pure water, 1.0 mM $CuCl_2$, and $Cu(NO_3)_2$ solutions, respectively. However, no fibers in this category are found in 1.0 mM $CuSO_4$ solution. Instead, 94% of fibers formed in this solution have a length longer than 1000 nm. The fiber lengths obtained in the presence of the three copper salts are affected by the anion in the following order: $SO_4^{2-} \gg NO_3^- \geq Cl^-$.

To investigate if the observed anion effect occurs in salt solutions without copper, we conducted a series of control experiments in which 0.025 mg mL^{-1} peptide was dissolved in 1.0 mM Na_2SO_4 and NaCl rather than the corresponding copper salts. As shown in Figure 6, EAK16(II)GGH formed a network of short fibers, not long fibers, in the presence of NaCl and Na_2SO_4. In addition, there is no significant difference in the structure formed depending on whether Cl^- or SO_4^{2-} is present. This observation shows that the presence of Cu^{2+} is important for the anion effect on the peptide self-assembled nanostructures.

Effect of Salt Concentration on Nanostructures. Figure 7 presents the nanostructures obtained in 0.05 mg mL^{-1} EAK16-(II)GGH solutions in the absence of a copper salt (Figure 7a) and at different $CuSO_4$ concentrations (Figure 7b−e). The peptide forms short fibers and a few small aggregates in pure water (Figure 7a), but longer fibers are observed in the presence of

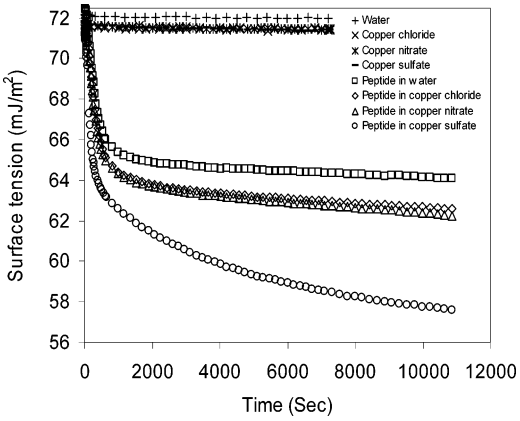

Figure 10. Dynamic surface tension of pure water, copper salts, and 0.05 mg mL^{-1} EAK16(II)GGH with and without copper salt solutions.

copper sulfate. The fiber length was found to depend on the concentration of copper sulfate (Figure 7b−e). The dimensions of the peptide fibers are shown in Table 1. The average widths of the peptide fibers vary from 50 to 60 nm, whereas the average heights vary from 0.5 to 1.0 nm, both independent of copper sulfate concentration. The statistical analysis (Figure 7f) shows that 80% of fibers formed in pure water are very short (<300 nm). In 0.05 mM $CuSO_4$ solution, only 12% of fibers are very short, but 82% of fibers have a length ranging from 300 to 1000 nm; few fibers (6%) are longer than 1000 nm. With an increase of copper sulfate concentration from 0.05 to 10.0 mM, the population of fibers with a length above 1000 nm increases from 6% to 94%. When the copper sulfate concentration is above 1.0 mM, the peptide forms long fibers almost exclusively.

The nanostructures found in 0.05 mg mL^{-1} EAK16(II)GGH solutions containing $CuCl_2$ (0.05−10.0 mM) consist predominately of very short fibers (Figure 8a−d). No long fibers (>1000 nm) are observed over the salt concentration range studied. The width and height of these fibers are independent of $CuCl_2$ concentration, as shown in Table 1. The fiber width and height are found to be ∼60 nm and ∼0.5−1.0 nm, respectively. The statistical analysis shows that ∼80% of fibers have a length below 300 nm over the $CuCl_2$ concentration range of 0.05−10.0 mM (Figure 8e). Similar behavior is observed in $Cu(NO_3)_2$ solutions, with very short fibers being evident at both 0.05 and 10.0 mM concentrations (Figure 9a,b). The fiber width and height are found to be ∼50 nm and ∼0.5−1.0 nm, respectively (Table 1). Although the population of short fibers (300−500 nm) slightly increases at a higher $Cu(NO_3)_2$ concentration of 10.0 mM, the predominant population of fiber length is still below 300 nm at concentrations of 0.05 (86%) and 10.0 mM (76%) (Figure 9c).

Effect of Anion on Surface Tensions of EAK16(II)GGH Solutions. Surface tension measurements can give information on the amphiphilicity of the peptide and the nature of its self-assembly in different copper salt solutions. The greater the peptide amphiphilicity, the greater its activity at the air−liquid interface and the lower its surface tension. Figure 10 shows the variation of surface tension with time for 0.05 mg mL^{-1} EAK16(II)GGH in salt-free solution and in the presence of 1.0 mM copper salts. The surface tensions of the control samples, including pure water and 1.0 mM copper salt solutions, remain constant (∼72 mJ m^{-2}) over 2 h. For peptide solutions with and without copper salts, the surface tensions decrease rapidly at the outset before leveling off and slowly approaching equilibrium. The equilibrium surface tension values were calculated based on the average over the last 10 points of data. The peptide has an equilibrium surface tension value of 64.1 mJ m^{-2} in pure water. The presence of the copper salts causes the surface tension to decrease to a level that depends on the salt type. Once again, the behavior in $CuSO_4$ solution appears to stand out from that observed in the other two copper salt solutions. The equilibrium surface tensions of the peptide in $CuCl_2$ and $Cu(NO_3)_2$ solutions are 62.6 and 62.2 mJ m^{-2}, respectively, but only 57.6 mJ m^{-2} in the presence of $CuSO_4$. These results indicate that the surface activity of peptide self-assemblies in different copper salt solutions depends on the anion type in the following order: $SO_4^{2-} > NO_3^- \geq Cl^-$. Although the equilibrium surface tension value of the peptide in the presence of $CuCl_2$ is only slightly higher than in the presence of $Cu(NO_3)_2$, this trend is consistently observed in repeated experiments.

Discussion

Peptide Design and Secondary Structure in the Absence of Copper Salts. EAK16-II, the molecular motif for EAK16-(II)GGH, is an ionic-complementary peptide which has been well studied and shown to form a β-sheet structure in pure water.[28] It is expected that the secondary structure of EAK16-II is formed through hydrogen bonding and stabilized by hydrophobic and electrostatic interactions. However, with the addition of the short metal ion binding group GGH at the C-terminus, the peptide EAK16(II)GGH has been found to form a predominantly α-helix/random coil structure (Figure 4), suggesting that the GGH group located at the C-terminus affects the secondary structure of the peptide. One possible reason for this phenomenon is that the introduction of the GGH group reduces the ionic-complementary character on the C-terminal side of the peptide. This makes it more difficult for the peptide to self-assemble into β-sheets than in the case of the more ionic-complementary EAK16-II. Another contributing factor may be the presence of the glycine residue introduced by the modification of the peptide. Since the glycine residue is the shortest among all amino acids, its presence may increase the backbone flexibility of the peptide chain and disrupt the β-sheet secondary structure. It has been reported that the replacement of alanine by glycine can hinder the formation of β-sheets.[41] Although the modification causes a change in the secondary structure, it should be emphasized that the modified peptide can still self-assemble into nanofibers, only to a less extent.

Effect of Anion on the Secondary Structure of EAK16-(II)GGH. The secondary structure of a peptide molecule in solution can be affected by the solution composition.[42−45] Our FTIR spectra show that the secondary structure of EAK16(II)-GGH is affected by the presence of the copper salts containing different anions (Figure 4). In the presence of sulfate, the peptide predominantly forms β-sheets. However, in the presence of chloride and nitrate anions, the peptide forms a mixture of α-helices/random coils and β-sheets. The observed anion effect on EAK16(II)GGH may be due to the different valence of anions. The divalent sulfate anion may serve as a bridge to link two peptide molecules by interacting with two positively charged lysine residues. Such an intermolecular interaction may bring the two peptide molecules together, promoting the formation of β-sheets. Monovalent anions (i.e., chloride and nitrate) cannot function as bridges, and so their primary effect may be to shield the charges on peptide molecules electrostatically. This shielding

(41) Petty, S. A.; Adalsteinsson, T.; Decatur, S. M. *Biochemistry* **2005**, *44*, 4720−4726.
(42) Zhong, L.; Johnson, W. C. *Proc. Natl. Acad. Sci. U.S.A.* **1992**, *89*, 4462−4465.
(43) Mutter, M.; Hersperger, R. *Angew. Chem., Int. Ed. Engl.* **1990**, *29*, 185−187.
(44) Mutter, M.; Gassmann, R.; Buttkus, U.; Altmann, K.-H. *Angew. Chem., Int. Ed. Engl.* **1991**, *30*, 1514−1516.
(45) Waterhous, V. D.; Johnson, W. C. *Biochemistry* **1994**, *33*, 2121−2128.

may still facilitate β-sheet formation, but not to the extent with a "bridging agent" such as sulfate. Therefore, a mixed secondary structure was observed in copper chloride and copper nitrate solutions. Preliminary molecular dynamic simulations (see the Supporting Information) also confirm the effect of sulfate and chloride on the peptide secondary structure. These calculations indicate that a β-sheet structure is more favored in the presence of sulfate than in the presence of chloride, a trend that agrees with our experimental results.

Effect of Anion on the Self-Assembled Nanostructure of EAK16(II)GGH. Our results show that the self-assembled nanostructure of EAK16(II)GGH in aqueous solution depends significantly on the particular anion present. Sulfate can induce long fiber formation, whereas chloride and nitrate cannot. This phenomenon is observed at different peptide concentrations (0.025 and 0.05 mg ml^{-1}) and over salt concentrations ranging from 0.05 to 10.0 mM (Figures 5 and 7-9). Anions have been previously shown to increase or decrease the pK_a of histidine by 0.1 to 0.3 pH unit depending on the location of histidine on a peptide chain and the type of anion present.[32] A change in the pK_a value of histidine could affect the amount of copper binding to the peptide. However, our UV−vis titration and nuclear magnetic resonance (NMR) results show that the type of anion does not affect the amount of copper binding to the peptide (Figures 2 and 3). This indicates that our observed anion effect may not be due to differences in the extent of copper binding.

The divalent SO_4^{2-} anion may bridge the peptide molecules through the electrostatic interaction with the positively charged residues from two peptide molecules similar to the role of divalent cations in DNA condensation.[46] Many multivalent cations have been found to be more efficient than monovalent cations in inducing the condensation and fiber formation of DNA and other synthetic polyelectrolytes.[47,48] It has been reported that when the size of a divalent cation is much smaller than the space between two neighboring negatively charged residues along a polyelectrolyte chain, the primary effect of the divalent cation may not be to electrostatically interact with the charges from these two residues; instead, it is more likely for the cation to interact with one negative residue of one chain and one negative residue of another chain and bring about the onset of condensation.[49] A similar effect may explain the influence of sulfate on the positively charged residues of EAK16(II)GGH. The minimum spacing between two positive residues on EAK16(II)GGH is greater than 7.3 Å (estimated from Chemsketch software without optimization), which is considerably larger than the sulfate ionic radius of 2.9 Å.[50] Thus, it is not likely that the divalent anion can interact with the two neighboring lysine residues on a single peptide. Instead, it may electrostatically interact with one positive lysine residue of one peptide molecule and serve as a sticky point for a positive lysine residue of a second peptide molecule. In this way, sulfate facilitates the peptide molecules to interact with one another. Such intermolecular attraction might greatly favor β-sheet formation of EAK16(II)GGH (Figure 4). The extensive β-sheet formation may cause the peptide to form long fibers due to the growth in the direction perpendicular to the β strands or the interaction between β-sheets. On the other hand, monovalent chloride and nitrate anions may not have such a bridging capability, so the peptide secondary structure contains mixed α-helices/random coils and β-sheets in copper chloride and copper nitrate solutions. These mixed structures may prevent long fiber formation, causing the peptide to self-assemble to short fibers and small aggregates, similar to that observed in pure water. A very preliminary model of peptide self-assembly and fiber growth is proposed in the Supporting Information.

It should be noted that the binding of copper to the peptide may play an important role in the way that the anion affects the peptide nanostructures. The self-assembled EAK16(II)GGH nanostructures formed in sodium salt solutions were similar, regardless of the anion type present as shown in Figure 6. This suggests a close relationship between the binding of Cu^{2+} to the peptide and the effect of anions on the self-assembled nanostructures. We investigated this question further by carrying out experiments to compare the effects of the different copper and sodium salts on the self-assembled nanostructures of EAK16-II, which does not contain a specific copper binding moiety (see the Supporting Information). Once again, the specific anion present had no effect on the self-assembled nanostructures. These results provide strong support that the copper binding to the peptide is pivotal to the effect of the different anions on EAK16(II)GGH nanostructures.

Surface Activity of Peptide Assemblies in Copper Salt Solutions. The change in the morphology of peptide self-assembled nanostructures due to the presence of the different anions was also studied from surface tension measurements. The peptide solution exhibits a lower surface tension in the presence of sulfate than that of the other two anions. Experiments conducted with the copper salt solutions without peptide show that the surface tensions of different salts are very similar to each other and to that of pure water ($\sim$72 mJ m^{-2}). The different surface tensions shown in Figure 10 are therefore likely due to amphiphilicity changes of the peptide self-assemblies in the presence of the different anions. According to the order of surface tension values of the peptide in different copper salt solutions, the amphiphilicity of the peptide self-assemblies may decrease depending on anion type in the following order: $SO_4^{2-} > NO_3^- \geq Cl^-$. This order correlates well with the variation of the β-sheet content in the peptide secondary structure (Figure 4).

A characteristic feature of an EAK16(II)GGH molecule is that most of its hydrophobic (●) and hydrophilic (○) residues are arranged in an alternating pattern ●○●○●○●○●○●○●○●○●●○, except at the GGH end. Such an alternating pattern in a β-strand will result in a unique structure: hydrophilic residues on one side of the peptide chain and hydrophobic residues on the other side.[51] Thus, β-sheets containing this unique structure are predominantly amphiphilic and tend to move to an air−water interface. The orientation of the β-sheets with the hydrophobic side facing the air and the hydrophilic side directed into the aqueous solution would result in a lower surface tension. On the other hand, since α-helix/random coil structures of EAK16(II)GGH do not have such a unique amphiphilic feature, they may not have the same surface activity as a β-sheet structure does. This last comparison may explain our finding that the order of the surface activity in different copper salts correlates well with the β-sheet content in the secondary structure of peptide self-assembled nanofibers (Figures 4 and 10).

Conclusions

EAK16(II)GGH peptide capable of binding with Cu^{2+} has been successfully designed by adding a GGH group to the

(46) Dahlgren, P. R.; Lyubechenko, Y. L. *Biochemistry* **2002**, *41*, 11372−11378.
(47) Sun, X.-G.; Cao, E.-H.; Zhang, X.-Y.; Liu, D.; Bai, C. *Inorg. Chem. Commun.* **2002**, *5*, 181−186.
(48) Korolev, N.; Lyubartsev, A. P.; Rupprecht, A.; Nordenskiöld, L. *Biophys. J.* **1999**, *77*, 2736−2749.
(49) Butler, J. C.; Angelini, T.; Tang, J. X.; Wong, G. C. L. *Phys. Rev. Lett.* **2003**, *91*, 28301.
(50) Nightingale, E. R., Jr. *J. Phys. Chem.* **1959**, *63*, 1381−1387.
(51) Xu, G.; Wang, W.; Groves, J. T.; Hecht, M. H. *Proc. Natl. Acad. Sci.* **2001**, *98*, 3652−3657.

C-terminus of the peptide EAK16-II. The binding of Cu^{2+} to the histidine group of the peptide has been confirmed by ^1H NMR and UV−vis absorption spectroscopy. The effect of the anions SO_4^{2-}, Cl^-, and NO_3^- in solution on peptide self-assembly was investigated using AFM, surface tension measurement, and FTIR spectroscopy. The experimental results suggest that the type of the anion has a significant effect on the EAK16(II)GGH secondary structure, self-assembled nanostructures and surface activity over a range of peptide and salt concentrations. The length of peptide nanofibers, the β-sheet content, and the surface activity increase according to the type of the anion present in the following order: $SO_4^{2-} > NO_3^- \geq Cl^-$. The divalent SO_4^{2-} may serve as a bridge linking two peptide molecules resulting in the formation of long fibers.

Our study showed that the dimension of EAK16(II)GGH self-assembled nanostructures can be controlled by adding copper salts with different types of anions. Sulfate induces long fiber formation, whereas chloride and nitrate cause short fiber formation. This may be important for different applications in nanotechnology, especially for metallic nanowire fabrication. By controlling the dimension of a peptide template, desired dimensions of the fabricated nanowire may be obtained. Furthermore, the successful design of peptide EAK16(II)GGH with the combined properties of fiber formation and metal ion binding capability provides a simple way to create functional biological materials and provide a simple model for metal ion binding proteins such as prion and β-amyloid proteins.

Acknowledgment. We thank Drs. Yooseong Hong, Liz Meiering and Neil McManus for helpful discussions. We also thank Janet Venne for help with the NMR experimental work. Support for this research has been provided by the Natural Sciences and Engineering Research Council of Canada (NSERC), Canada Foundation for Innovation (CFI), and the Canada Research Chairs (CRC) Program for one of the coauthors (P.C.).

Supporting Information Available: Computer simulation work of the anion effect on the self-assembling peptide EAK16(II)GGH, the effect of sodium salts and copper salts on the self-assembled nanostructures of EAK16-II, and a preliminary model of EAK16(II)GGH self-assembly in copper salt solutions. This material is available free of charge via the Internet at http://pubs.acs.org.

LA061238P